

# Effects of filler material on the characteristics of electrospun polyvinyl alcohol/Nafion nanofibrous membranes

Mert Işlay<sup>1,2</sup>  | Ahmet Çay<sup>3</sup>  | Çiğdem Akduman<sup>4</sup>  |  
Emriye Perrin Akçakoca Kumbasar<sup>3</sup>  | Hasan Ertaş<sup>5</sup> 

<sup>1</sup>Department of Textile Engineering, Graduate School of Natural and Applied Sciences, Ege University, Bornova, İzmir, Türkiye

<sup>2</sup>Department of Textile Engineering, Faculty of Engineering, Dokuz Eylül University, Buca, İzmir, Türkiye

<sup>3</sup>Department of Textile Engineering, Faculty of Engineering, Ege University, Bornova, İzmir, Türkiye

<sup>4</sup>Department of Textile Technology, Denizli Vocational School of Technical Sciences, Pamukkale University, Denizli, Türkiye

<sup>5</sup>Department of Chemistry, Faculty of Science, Ege University, Bornova, İzmir, Türkiye

## Correspondence

Ahmet Çay, Department of Textile Engineering, Faculty of Engineering, Ege University, Bornova, İzmir, Türkiye.  
Email: [ahmet.cay@ege.edu.tr](mailto:ahmet.cay@ege.edu.tr)

## Funding information

Ege University Research Foundation, Grant/Award Number: FYL-2019-21411

## Abstract

In this study, polyvinyl alcohol/Nafion nanofibrous composite membranes were produced to investigate their possible application as a polymer electrolyte membrane (PEM) in direct methanol fuel cells. Electrospinning method was used for nanofibrous membrane production, in which the mixture of polyvinyl alcohol (PVA) and Nafion solutions was directly electrospun. Produced nanofibers were subjected to physical stabilization, filler application, and sulfonating to produce composite nanofibrous membranes. PVA and Nafion polymers were used also as filler materials. The properties of resultant composite membranes were compared in terms of water swelling, weight loss in water and methanol solution, thermal stability, morphology, proton conductivity, and methanol permeability. Proton conductivity of the membranes depending on the humidity was also investigated. TGA analysis showed that the membranes had adequate thermal properties regardless of the filler material. The nanofibrous structure was shown to be preserved by scanning electron microscopy (SEM) after treatment with water and methanol solution. It was shown that PVA/Nafion nanofibers displayed proton conductivity after filling process. The use of PVA as a filler material led to higher proton conductivity at 100 RH %. It was reported that proton conductivity could only be obtained at higher relative humidity values (>80% RH). A lower methanol permeability of PVA-filled membranes was reported.

## Highlights

- PVA/Nafion nanofibrous membranes were produced by electrospinning.
- PVA and Nafion were also used as pore filling materials.
- PVA-filled membranes had higher proton conductivity and lower methanol permeability.
- Proton conductivity could only be obtained at higher RH% values.

## KEYWORDS

electrospinning, filler, Nafion, nanofiber, polymer electrolyte membrane, polyvinyl alcohol

## 1 | INTRODUCTION

The energy needs have been mainly provided by combustion of fossil fuels, which has increased the air pollution and the emission of CO<sub>2</sub>. This has disrupted the balance in nature and caused several ecological problems.<sup>1</sup> The utilization of renewable energy resources is now more crucial than ever to achieve a sustainable world. Not only do renewable energy resources support environmental sustainability but they also contribute to the fight against climate change by reducing greenhouse gas emissions into the atmosphere.<sup>2</sup> With advancing technology, it is now possible to manufacture environmentally friendly, safe, and efficient devices. Fuel cells are considered one such example.<sup>3</sup> A fuel cell is an electrochemical device that converts the chemical energy of a fuel and an oxidizing agent directly into electrical energy.<sup>4</sup> It is a type of renewable energy technology that offers an alternative to traditional combustion-based power generation. Fuel cells operate through an electrochemical reaction between hydrogen (or a hydrogen-rich fuel) and oxygen (from the air).<sup>5</sup> The basic components of a fuel cell are an anode (negative electrode), a cathode (positive electrode), and an electrolyte, which facilitates the movement of ions between the anode and cathode.<sup>6</sup>

There are different types of fuel cells, categorized based on the type of electrolyte used. Common types include proton exchange membrane fuel cells (PEMFC), solid oxide fuel cells (SOFC), alkaline fuel cells (AFC), and molten carbonate fuel cells (MCFC). Polymer electrolyte membrane fuel cells (PEMFC) have emerged as a leading energy conversion technology for stationary, transportation, and portable electronic applications. The popularity of PEMFCs as an alternative power source is attributed to their low-temperature operation (<100°C), high efficiency, fast start-up, and shutdown cycles, and low emission and noise.<sup>7,8</sup>

PEMFCs are a popular type of fuel cell; however, researchers highlight that, despite their efficiency and environmental friendliness, certain scientific, technical, and economic challenges hinder their global commercialization and widespread use.<sup>9</sup> In PEMFCs, hydrogen is typically employed as fuel, but issues related to the storage and logistics of hydrogen have prompted the exploration of alternative fuels. Methanol, with advantages such as higher energy density than hydrogen, ease of storage, and convenience in liquid form, has gained attention. Consequently, direct methanol fuel cells (DMFCs), derived from PEMFCs and utilizing methanol as fuel, have emerged.<sup>10,11</sup>

The most popular and commercially available membranes used as PEM in fuel cells are perfluorosulfonic acid membranes, such as Nafion. Nafion is known for its superior mechanical strength, stability, and high-proton conductivity.<sup>12</sup> Examining its chemical structure

reveals a backbone of hydrophobic fluorocarbon chains alongside hydrophilic sulfonic acid groups. The sulfonic acid groups in its structure are responsible for the proton conductivity, and the higher proton conductivity is directly proportional to the abundance of water content in the structure.<sup>13</sup> However, its high cost, low proton conduction at elevated temperatures leading to dehydration, and methanol permeability negatively impact fuel cell performance.<sup>14,15</sup> Due to challenges encountered with traditional fuel cell membranes, research efforts have shifted toward the development of alternative membranes. Among these endeavors, the development of nanofibrous composite membranes has garnered significant attention in recent years.

Nanofibers possess notable characteristics including a high surface area and advanced physical and mechanical properties making them versatile for various applications.<sup>16,17</sup> Presently, the electrospinning method, which utilizes high molecular weight polymers and facilitates easier and simpler production, has gained prominence for nanofiber production.<sup>18</sup> The utilization of nanofibers in polymer electrolyte membranes has gained significant attention because of the creation of extended proton conduction channels within the membrane. Yao et al.<sup>19</sup> developed composite sulfonated polystyrene (SPS)/Nafion membranes by impregnating SPS nanofibers with Nafion solution and highlighting a substantial increase in proton conductivity attributed to the abundance of ionic groups on the nanofiber surface. Similarly, studies by Yao et al.<sup>20</sup> and Takemori and Kawakami<sup>21</sup> revealed that the incorporation of nanofibers into the membrane structure enhances proton conductivity. These studies collectively demonstrate the utility of nanofibers in augmenting proton conductivity.

Within the scope of this study, efforts were made to produce Nafion nanofibers and develop composite proton-conducting membranes using these nanofibers. However, nanofibers cannot be produced solely from a Nafion polymer solution using electrospinning. To achieve this, a carrier polymer is required. Literature review revealed that polymers such as polyethylene oxide,<sup>22–24</sup> polyvinyl alcohol,<sup>23,25,26</sup> polyphenyl sulfone,<sup>27</sup> polyacrylic acid,<sup>28</sup> and polyvinyl pyrrolidone<sup>25</sup> have been employed as carrier polymers.

In this study, polyvinyl alcohol (PVA) was chosen as a carrier polymer, considering the ease of electrospinnability, stabilization by crosslinking, and its ability to be sulfonated to contribute to proton conduction. According to the literature, studies involving the use of PVA polymer follow a common procedure for the production of Nafion/PVA nanofibrous membranes, where initially PVA nanofibers were produced, and subsequently, after crosslinking and sulfonating processes, composite membranes were obtained by impregnation with a Nafion solution.<sup>29–31</sup>

For instance, Mollá and Compañ<sup>9</sup> produced PVA nanofibers using the electrospinning method. To enhance the proton conductivity, sulfonation was conducted with 4-formyl-1,3-benzenedisulfonic acid disodium salt (FBDA). The sulfonated PVA nanofibers were subsequently impregnated with a Nafion solution. The resulting composite membrane exhibited a proton conductivity of 0.022 S/cm in an aqueous environment at 70°C. It was reported that PVA/Nafion composite membranes demonstrated comparable performance to the Nafion film membrane in DMFC. It was emphasized that the nanofibrous structure contributes to an improvement in methanol permeability and may present a more economical alternative. Lin et al.<sup>32</sup> impregnated PVA nanofibers with a Nafion solution after crosslinking them with glutaraldehyde. The resulting composite membrane was reported to be thinner (approximately 1/3 the thickness) than the commercial Nafion 117 membrane. Moreover, it was highlighted that the DMFC fuel cell performance improved due to the lower methanol permeability of the composite membrane. These studies indicated an enhancement in the methanol permeability of Nafion-filled PVA nanofiber membranes. Notably, there is a gap in the literature concerning the impact of Nafion presence in nanofiber form on fuel cell performance. The potential use of PVA/Nafion nanofibers for fuel cell applications has only appeared in our previous study, in which the stability assessment of the PVA/Nafion nanofibers was investigated for the use in DMFCs.<sup>33</sup> The produced nanofibers were compared according to the stabilization methods of PVA and concluded that thermally stabilized PVA/Nafion nanofibers had the highest stability. However, proton conductivity and methanol permeability of those membranes were not tested. In the present study, PVA was chosen as the carrier polymer, and unlike other studies in the literature, the objective was to create a nanofibrous structure by employing electrospinning after combining PVA and Nafion during the solution preparation stage. The novelty of this study is the investigation of methanol permeability and proton conductivity of the PVA/Nafion-based nanofibrous composite membranes. For the first time in the literature, the impact of using Nafion or PVA as filler on the properties was examined. Furthermore, the effect of humidity on proton conductivity of PVA/Nafion nanofibrous composite membranes was also presented and discussed.

## 2 | EXPERIMENTAL

### 2.1 | Materials

PVA (Mowiol<sup>®</sup> 20–98, 125,000 g/mol), Nafion<sup>®</sup> 117 solution (~5% in a mixture of lower aliphatic alcohols and water), 4-formylbenzene-1,3-disulfonic acid disodium

salt hydrate (FBDA) and Tween 80<sup>®</sup> (polyoxyethylene sorbitan monooleate) were purchased from Sigma-Aldrich. Isopropanol (99.5%), hydrochloric acid (HCL, 37%), methanol (99.9%) and sulfuric acid (H<sub>2</sub>SO<sub>4</sub>, 95%–98%), sodium chloride (NaCl), sodium hydroxide (NaOH), hydrogen peroxide (H<sub>2</sub>O<sub>2</sub>, 50%), iron (II) sulfate (FeSO<sub>4</sub>·7H<sub>2</sub>O), and phenolphthalein indicator were also used in tests. All of these chemicals were used as is, without any further purification process.

### 2.2 | Electrospinning of PVA/Nafion nanofibers

To prepare the electrospinning solution, a 10% PVA aqueous solution was prepared by stirring at 80°C for at least 3 h. Based on the previous study,<sup>33</sup> the optimal mixing ratio of PVA and Nafion solutions for producing electrospun PVA/Nafion nanofibers was determined to be 1:1 by volume (corresponding to 1:0.5 w/w ratio for PVA:Nafion). Accordingly, the electrospinning solution was prepared by mixing the prepared PVA solution with a 5% Nafion solution at a 1:1 volume ratio (1:0.5 w/w ratio for PVA:Nafion). Tween 80<sup>®</sup> (a surfactant, polyoxyethylene sorbitan monooleate) was added at a rate of 0.05 mL/g<sub>polymer</sub> to reduce the surface tension.<sup>34,35</sup> Nanofibers were produced using an electrospinning device (Nanospinner, NS Plus, Inovenso), which includes a high-voltage power supply connected to the needle tips, two feeding units, and a collector unit that can function as a rotating cylinder or flat metal. For nanofiber production, 3.5 cm long and 22 gauge thick needles with blunt ends were employed. The electrospinning process was conducted on the prepared solutions, achieving the desired thickness with parameters set at 18 kV nanofiber spinning voltage, 15 cm distance between the needle and collector, and a flow rate of 0.7 mL/h. The nanofibers were collected on a flat metal collector covered with an aluminum foil. Produced nanofibrous membrane was heat treated at 180°C for 1 h in an oven to stabilize the PVA fraction in the structure.

### 2.3 | Filler material application

Since the produced nanofibrous membranes were porous, it was necessary to apply a filler to close the pores. PVA and Nafion were used as fillers. Accordingly, 5% PVA and 5% Nafion solutions were employed for the filling process. Five percent PVA solution (Mowiol<sup>®</sup> 20–98, 125,000 g/mol) was prepared by stirring at 80°C for 3 h. For the Nafion filling, a 5% Nafion 117 solution was used. PVA/Nafion nanofibers were immersed in the prepared solutions for 5 min; after which, the surface water was

removed by filter paper, and the impregnated membranes were dried in an oven at 80°C. This process was repeated 3 times for the filling to be smooth. The samples applied with the filler material were stabilized by heat treatment at 180°C for 1 h. Weight gain (%) after filling application was calculated according to Equation (1), where  $M_0$  is the weight of the neat membrane and  $M_c$  is the weight of the filled membrane.

$$\text{Weight gain} = \frac{M_c - M_0}{M_0} \times 100 \quad (1)$$

Nafion and PVA-filled samples were denoted as PVA/Nafion+PVA and PVA/Nafion+PVA, respectively.

## 2.4 | Sulfonating

The membranes were sulfonated for PVA fraction to demonstrate proton conductivity ability as well as the Nafion within the membrane structure. The membranes were immersed into 0.04 M FBDA and 0.1 M HCL in isopropanol/water (70:30 v/v) solution and kept at 60°C for 2 h. Subsequently, they were incubated in a mixture of isopropanol/water (70:30 v/v) containing 0.3 M HCL for 5 min. Finally, the membranes were washed with a mixture of isopropanol/water (70:30 v/v) and pure isopropanol for 5 min each. The samples were then dried at room temperature.<sup>36</sup>

## 2.5 | Tests and characterization

The morphology of the produced nanofibrous membranes was investigated using SEM (Thermo Scientific Apreo S). Each sample was subjected to gold plating with Leica EM ACE600 coating device before processing. The mean nanofiber diameter of PVA/Nafion nanofibers was determined using Image J software. They were measured by drawing lines perpendicular to the fiber axis on the SEM images. The pixel values of the lines were converted to diameter values. In each case, 50 measurements were carried out from different parts of the samples.

FTIR analysis was carried out using a PerkinElmer, Spectrum 100 FTIR spectrometer.

Polymer electrolyte membranes must exhibit temperature resistance for use in fuel cells. The thermal stability of PVA/Nafion-based nanofibrous composite membranes was determined by thermogravimetric analysis (TGA) (TA Instruments, SDT Q600) in a nitrogen environment, with a temperature increase rate of 10°C from room temperature to 600°C.

To determine the swelling and weight loss of the membranes in water, as well as the weight loss in

methanol solution, they were immersed in distilled water and 5 M methanol solution, respectively, at 80°C for 24 h. Subsequently, the membranes were removed, and their wet weights were measured after removing the water on their surfaces with filter paper. Weight loss (%) and swelling (%) values were calculated using Equation (2) and Equation (3), respectively, where  $M_0$  represents the initial dry weight,  $M_w$  is the wet weight after treatment with water, and  $M_1$  is the dry weight of the samples dried after treatment with water or methanol solution.

$$\text{Weight loss} = \frac{M_0 - M_1}{M_0} \times 100 \quad (2)$$

$$\text{Swelling} = \frac{M_w - M_1}{M_1} \times 100 \quad (3)$$

Fenton's reagent was used to test the oxidative stability of the samples. 3 ppm  $\text{Fe}^{+2}$  (using  $\text{FeSO}_4 \cdot 7\text{H}_2\text{O}$ ) was added into 3%  $\text{H}_2\text{O}_2$  solution and samples were immersed into the solution at 65°C for 24 h. Weight loss of the samples was calculated using Equation (2).

It has been noted that the water retention and ion exchange capacity (IEC) are correlated with the proton conductivity of the membranes. To conduct the IEC experiments in this regard, the membranes were immersed in a 1 M  $\text{H}_2\text{SO}_4$  solution and boiled for 1 h for protonation of the membranes,<sup>37,38</sup> followed by rinsing with boiling distilled water for 15 min and subsequent drying at room temperature. Afterward, a 2 M NaCl solution was prepared, and the membranes were immersed in these solutions for 48 h to facilitate the exchange of  $\text{H}^+$  and  $\text{Na}^+$  ions. After the incubation period, the membranes were removed from the solution and the remaining waste solution was titrated with 0.01 M NaOH solution using phenolphthalein as an indicator. Equation (4) was employed for the IEC calculation, where  $V_{\text{NaOH}}$  represents the volume of NaOH solution consumed during the titration until the color change,  $M_{\text{NaOH}}$  corresponds to the molarity of the NaOH solution, and  $W_0$  represents the dry membrane weight.<sup>27,30</sup>

$$\text{IEC} = V_{\text{NaOH}} \times M_{\text{NaOH}} / W_0 \quad (4)$$

Methanol permeability of the membranes was tested by using a diffusion cell (Side-Bi-Side-Cell, PermeGear). Prior to the methanol permeability test, each sample was immersed in distilled water for 24 h. Subsequently, the membranes were removed from the water and positioned between the diffusion cells, each comprising two parts with a 50 mL volume and a 1.5 cm diameter cell opening. One side contained pure water, while the other held a 2 M methanol solution. These liquids were stirred using

a magnetic stirrer during the test to ensure homogeneity. The test was conducted at a constant temperature of 25°C inside a climate chamber. Samples of 1.5 mL were extracted from the distilled water-filled side at specific intervals (30, 60, 90, and 180 min) and analyzed in GC-FID (Agilent Technologies 7820A) to determine methanol concentration. The methanol percentage of each sample was calculated based on chromatogram area values. Subsequently, using the obtained GC-FID data, methanol permeability was calculated with Equation (5), where  $DK$  ( $\text{cm}^2\text{s}^{-1}$ ) represents the methanol permeability coefficient,  $C_A$  (mol/L) and  $C_B$  (mol/L) denote the methanol concentration in diffusion cells,  $A$  ( $\text{m}^2$ ) is the membrane surface area,  $V_B$  (L) is the diffusion volume, and  $L$  (cm) is the membrane thickness.<sup>39</sup>

$$C_{B(t)} = AV_B^{-1}DKL^{-1}C_A(t - t_0) \quad (5)$$

Proton conductivity testing of the membranes was conducted using the Scribner 850e Fuel Cell Station. Prior to the proton conductivity test, the membranes were immersed in a 1 M  $\text{H}_2\text{SO}_4$  solution at room temperature for 24 h. The test was performed at 80°C under different relative humidity (40%, 60%, 80%, and 100% RH). Proton conductivity ( $\sigma$ , mS/cm) was calculated using Equation (6), where  $L$  (cm) represents the distance between the voltage probes (0.425 cm),  $W$  is the width (cm), and  $T$  is the membrane thickness (cm).

$$\sigma = L/(R \times W \times T) \quad (6)$$

## 3 | RESULTS AND DISCUSSION

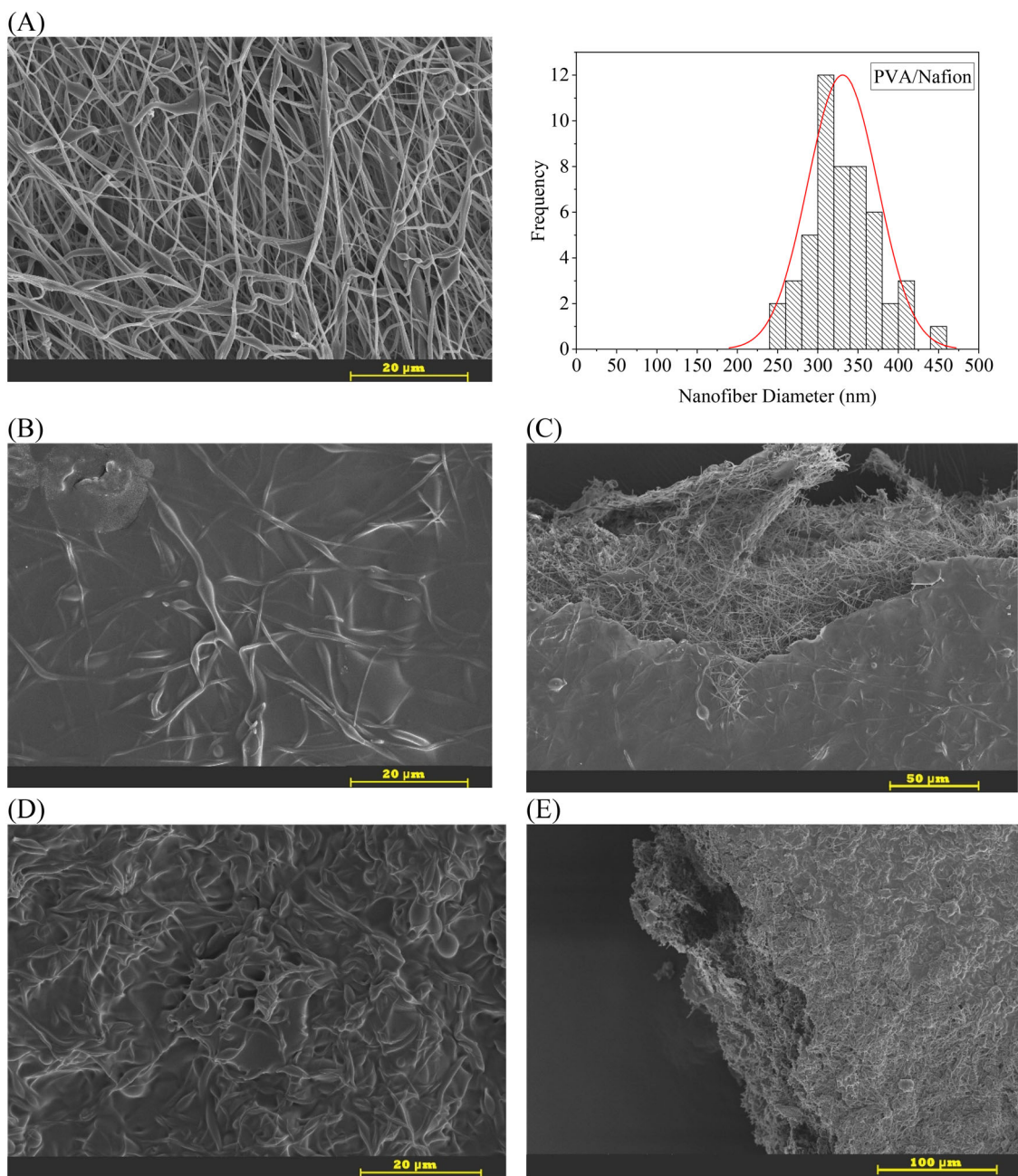
### 3.1 | Characterization of the membranes

Figure 1 illustrates the SEM images of the filler material applied to PVA/Nafion nanofibrous membranes and also displays the nanofiber diameter distribution histogram of PVA/Nafion nanofibers. The mean diameter of neat PVA/Nafion nanofibers was about 330 nm, and the nanofiber diameters were in the range of 250–450 nm as shown in the histogram, which shows that there was not a high deviation from the average nanofiber diameter. It is quite evident from the figure that the membranes filled with PVA exhibited a smoother surface. Conversely, the Nafion filler permeated into the membrane, while the PVA filler predominantly remained on the surface. This observation was likely attributed to the higher viscosity of the PVA solution, owing to the elevated molecular weight of PVA. The weight gain after the

filling process further supported this, which was 26.8% for PVA and 44.6% for Nafion filling. Since the PVA filler did not deeply penetrate the membrane, the weight gain remained lower. On the other hand, a higher weight gain was observed with the Nafion filler.

FTIR transmittance spectra of PVA/Nafion nanofibers, PVA and Nafion-filled PVA/Nafion nanofibers and Nafion 115 membrane are illustrated in Figure 2 in expanded regions of 3000–4000  $\text{cm}^{-1}$  and 650–1500  $\text{cm}^{-1}$  wavenumber. In order to carry out a deep understanding of the structure, FTIR spectra of PVA/Nafion nanofibers after electrospinning, after heat treatment for physical stabilization of PVA, and after sulfonating process were given in the figure. In the spectrum of Nafion 115 membrane, typical peaks at 1202  $\text{cm}^{-1}$  and 1143  $\text{cm}^{-1}$  are attributed to asymmetric and symmetric stretching of C-F bonds, and at 1054  $\text{cm}^{-1}$  associated with the sulfonic acid groups.<sup>40,41</sup> The band located at  $\sim 3460$   $\text{cm}^{-1}$  was associated with the hydroxyl groups of water that interact with the sulfonic acid groups.<sup>14</sup> In PVA/Nafion nanofibers, it was observed that the FTIR spectra were dominated by the typical Nafion bands. However, the peak at 1097  $\text{cm}^{-1}$  attributed to the secondary alcohol groups of PVA<sup>36</sup> is still visible at the spectra of PVA/Nafion nanofibers after electrospinning without any further treatment (the spectra of PVA/Nafion). The intensity of this peak was shown to be reduced after the heat treatment, which is thought to be because of the interaction of the –OH groups of PVA with the – $\text{SO}_3\text{H}$  groups of Nafion. Another indication of this interaction is the shifting of the O-H peak of PVA/Nafion nanofibers at 3310  $\text{cm}^{-1}$  to higher wavenumber (3379  $\text{cm}^{-1}$ ) after heat treatment. In the study of Kim et al.<sup>42</sup> the same shift was attributed to the hydrogen bonding interaction of –OH groups of PVA and – $\text{SO}_3\text{H}$  groups of PSSA, therefore, in this case, the same situation can be attributed to the interaction between Nafion and PVA. Deluca and Elabd<sup>14</sup> also approached that shifting of the –OH peak of Nafion to lower wavenumbers in PVA/Nafion nanofibers might be because of the aforementioned hydrogen bonding interaction.

Since the PVA/Nafion spectra was dominated by the peaks of Nafion, the addition of extra sulfonic acid groups by the sulfonation of PVA was not visible, due to overlapping. On the other hand, it was observed that the peak at 1096  $\text{cm}^{-1}$  corresponded to the secondary alcohol groups of PVA was disappeared after sulfonating process (when the spectra of PVA/Nafion-HT and PVA/Nafion-HT + S were compared), which was an indication of the successful sulfonation of –OH groups of PVA. This was also valid for the spectrum of PVA and Nafion-filled PVA/Nafion nanofibers, where sulfonation process was also applied. The spectrum of PVA and Nafion-filled PVA/Nafion nanofibers were similar to the spectra of sulfonated



**FIGURE 1** SEM images of (A) neat PVA/Nafion with nanofiber diameter distribution histogram, (B) PVA-filled PVA/Nafion, (C) Nafion-filled PVA/Nafion nanofibrous membranes, (D) cross-sectional view of PVA-filled membrane, (E) cross-sectional view of Nafion-filled membrane.

PVA/Nafion nanofibers; however, the intensity of Nafion based peaks were higher for Nafion-filled PVA/Nafion nanofibers possibly because of the increased amount of Nafion on the surface of the membranes.

TGA was carried out to assess the thermal resistance of PVA/Nafion nanofibrous membranes filled with PVA and Nafion. For comparison neat PVA/Nafion and commercial Nafion 115 membrane was also investigated. TG and DTG curves of these membranes are illustrated in Figure 3. The values of onset temperature of degradation

( $T_i$ ), peak degradation temperature ( $T_{max}$ ), half decomposition temperature ( $T_{1/2}$ ), and the fraction of char are given in Table 1. The weight loss observed below 100°C was attributed to the removal of moisture from the membranes. Notably, membranes filled with PVA exhibited higher weight loss in this region, indicating a greater moisture content due to the higher PVA fraction, which behaves also a physically stabilized hydrogel.

The Nafion 115 membrane was thermally stable up to nearly 300°C ( $T_i = 307^\circ\text{C}$ ). The degradation of most of

**FIGURE 2** FTIR spectra of PVA/Nafion nanofibrous membranes and Nafion 115 membrane (HT: After heat treatment, HT + S: After heat treatment followed by sulfonating).

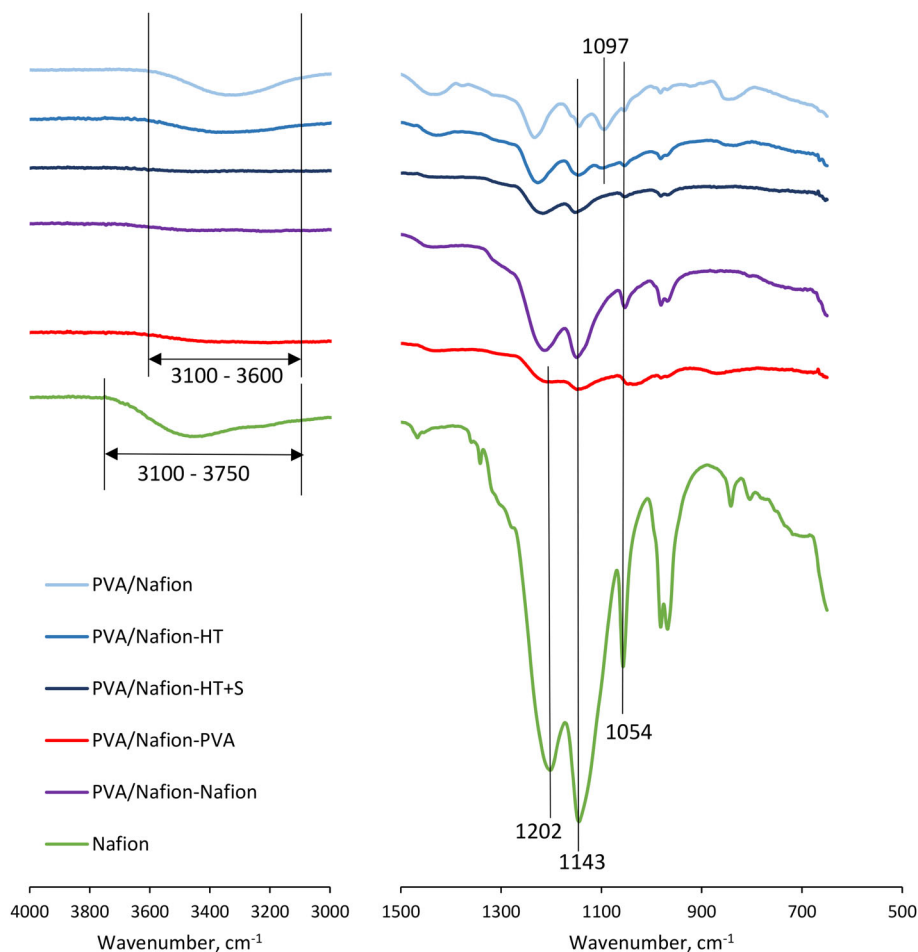
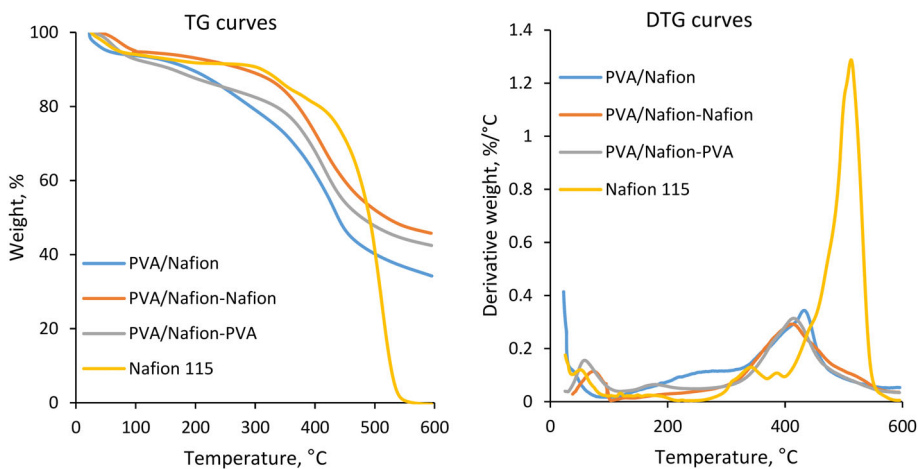


**FIGURE 3** TG and DTG curves of PVA/Nafion nanofibrous membranes and Nafion 115.



the sulfonic acid groups due to the decomposition of Nafion side chains started around 300°C, and the breakdown of the polymer backbone and residual sulfonic acid groups started around 400°C.<sup>43</sup> On the other hand, a slight decomposition was started at around 150°C for neat PVA/Nafion nanofibers possibly removal of the sulfonic acid groups added into the structure through sulfonation process, but the main degradation was observed

between 200 and 400°C, due to elimination reactions and subsequent polymer backbone degradation of the PVA.<sup>44</sup> However, the high residual fraction of char of the PVA/Nafion nanofibers (Nafion 115 membrane's was zero) and the absence of a decomposition peak at around 500°C and above indicated that the Nafion backbone might be protected<sup>30</sup> either because of blending with PVA or being brought into a nanofibrous form. The same effect was also

TABLE 1 Values of thermogravimetric analysis of PVA/Nafion nanofibrous membranes and Nafion 115 membrane.

|                   | Onset temperature ( $T_i$ ), °C | Peak degradation temperature ( $T_{max}$ ), °C | Temperature of half decomposition ( $T_{1/2}$ ), °C | Fraction of char, % |
|-------------------|---------------------------------|--|---|---------------------|
| PVA/Nafion        | 154                             | 433  | 452   | 34.2                |
| PVA/Nafion+PVA    | 161                             | 414  | 478   | 42.5                |
| PVA/Nafion+Nafion | 268                             | 412  | 525   | 45.7                |
| Nafion 115        | 307                             | 513  | 503   | 0.0                 |

valid for Nafion and PVA-filled PVA/Nafion nanofibers. It was also observed that, PVA filling led to a decrease in the degradation rate up to 400°C, which end up with a higher temperature of half decomposition. Nafion filling, on the other hand, led to a higher increase in the stability of the membrane up to 400°C compared to PVA filling. In this temperature range, its behavior was similar to Nafion 115 membrane, due to the higher fraction of Nafion within the structure by Nafion filling. It was investigated that filling process led to an increase in the temperature of half decomposition and residual fraction of char compared to neat PVA/Nafion nanofibers. Here, the highest results belonged to the Nafion-filled sample. These results confirmed that Nafion filling prolonged degradation and reduced the weight loss compared to PVA filling, which is the result of the higher thermal stability of Nafion. The main outcome of TGA study is that the filling process increased the thermal stability compared to neat PVA/Nafion nanofibers. Although PVA-filled nanofibrous membranes showed lower thermal stability compared to Nafion-filled ones, it's worth noting that both membranes exhibit suitability for use in fuel cells concerning temperature resistance, especially considering the relatively low operating temperatures (50–120°C) applied in the targeted DMFC applications.

### 3.2 | Swelling and weight loss

The swelling percentage and weight loss in water and weight loss in methanol solution of PVA/Nafion nanofibrous composite membranes are given in Table 2. It was shown that the PVA-filled membrane exhibited a notably high swelling value. This observation is supported by SEM images in Figure 3. In contrast, the swelling value of Nafion-filled membranes was lower than that of neat membranes. When PVA filling is used alone, it displays physically stabilized hydrogel behavior, resulting in a high degree of swelling.<sup>45</sup> On the contrary, in the case of Nafion filling, it was believed that the observed lower swelling stems from both the reduction in the weight percentage of PVA in the final membrane and the potential

interaction between the added Nafion and the PVA within the membrane. This interaction could be the formation of hydrogen bonds between the hydroxyl groups in PVA and the sulfonic acid groups in Nafion, rather than between the hydroxyl groups in PVA itself.<sup>14</sup> Notably, all PVA/Nafion composite nanofibrous membranes exhibited higher water retention capacity compared to commercial Nafion membranes. Upon examining weight losses, it was found that the PVA-filled membrane exhibited the highest weight loss, while Nafion-filled membranes displayed lower weight loss compared to even neat membranes similar to their swelling behavior. This lower weight loss in the Nafion-filled membrane was attributed to the interaction between PVA and Nafion, as elucidated in the swelling value. Upon exposure to a methanol solution, it was observed that the weight loss was minimal, and the stability of the membranes in the methanol solution was enhanced by filler application.

Oxidative stability tests showed that Nafion filling improved the oxidative stability of PVA/Nafion nanofibers, whose weight loss value was close to the commercial Nafion 115 membrane. On the other hand, an increase in weight loss was observed when PVA was used as a filler material.

Figures 3 and 4 show the SEM images of the filled membranes after water and methanol solution treatments, respectively. It was observed that the filling layer on the surface of PVA and Nafion-filled membranes was slightly disintegrated after treatment with water, but the nanofibrous structure was preserved, although swollen and conjugated parts appeared. On the other hand, no significant change in the membrane structure was observed as a result of treatment with methanol solution (Figure 5).

### 3.3 | IEC, proton conductivity, and methanol permeability

It is crucial for the membrane in fuel cells to have low methanol permeability because methanol can lead to undesired reactions within the fuel cell. Low methanol permeability can enhance the efficiency of the fuel cell



TABLE 2 Swelling in water and weight loss data of PVA/Nafion nanofibrous membranes.

| Sample                        | Weight loss in water, % | Swelling in water, % | Weight loss in methanol solution, % | Weight loss in Fenton's reagent, % |
|-------------------------------|-------------------------|----------------------|-------------------------------------|------------------------------------|
| PVA/Nafion                    | 3.7                     | 84.8                 | 5.3                                 | 10.7                               |
| PVA/Nafion with PVA filler    | 10.1                    | 456.1                | 1.5                                 | 21.4                               |
| PVA/Nafion with Nafion filler | 2.5                     | 44.3                 | 2.4                                 | 8.6                                |
| Nafion 115                    | 1.3                     | 20.1                 | 2.7                                 | 6.2                                |

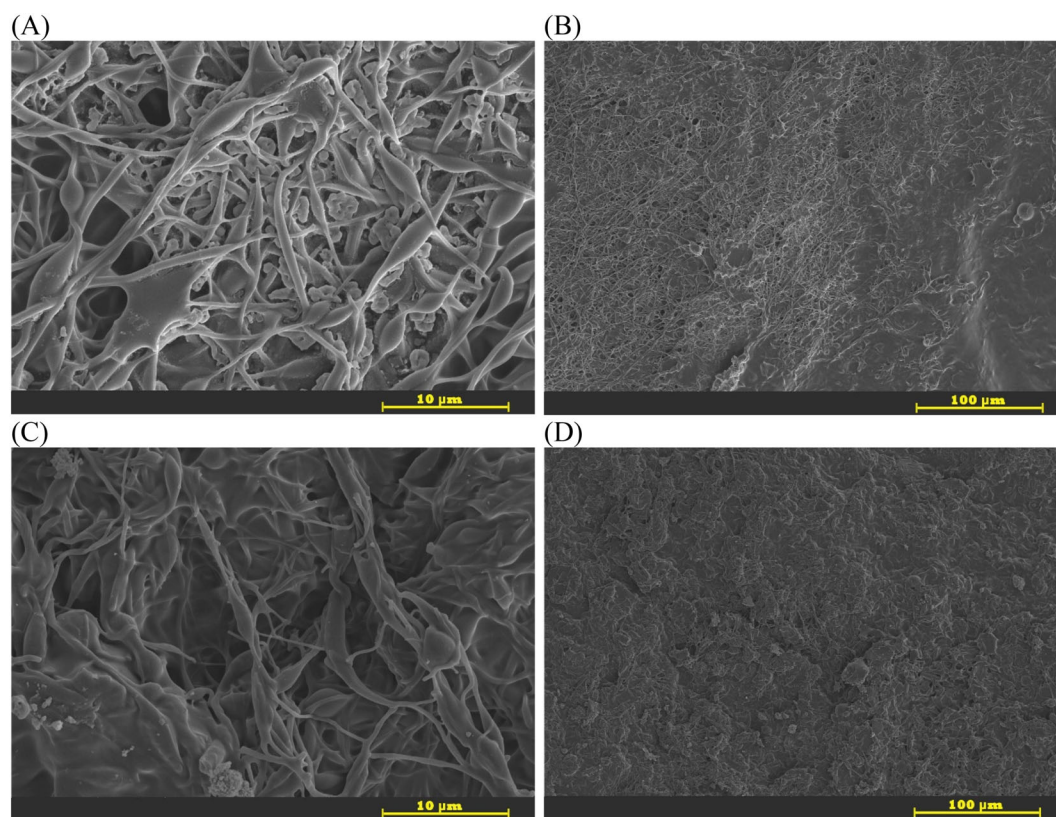


FIGURE 4 SEM images of (A, B) PVA-filled, (C, D) Nafion-filled PVA/Nafion nanofibrous membranes after water treatment.

and prevent unwanted methanol leaks. Besides, efficient transmission of protons in a fuel cell enhances the electrochemical reactions, contributing to overall efficiency. Good proton conductivity is essential for the fuel cell to generate sufficient power and improve performance. These two properties are utilized to assess the operational efficiency and durability of fuel cells. Ideally, a fuel cell membrane should possess high proton conductivity and low methanol permeability for optimal performance. Accordingly, IEC, methanol permeability, and proton conductivity properties of the produced PVA/Nafion nanofibrous composite membranes are given in Table 3.

IEC is related to the amount of ion-exchangeable groups and it affects the ionic conductivity and water

uptake of the membranes.<sup>46</sup> It was observed that PVA/Nafion nanofibers had lower IEC compared to Nafion membrane, although PVA/Nafion nanofibers had water uptake. This might be due to the lower sulfonic acid group content of PVA/Nafion nanofibers although an additional sulfonation process was applied. Another reason for lower IEC might be due decrease in the number of free sulfonic acid groups by the aforementioned interaction of Nafion and PVA after heat treatment. Both Nafion and PVA-filled samples demonstrated higher IEC values by the incorporation of additional sulfonic acid groups into the structure. The IEC of Nafion-filled membrane was higher possibly due to the incorporation of higher amounts of sulfonic acid groups into the structure

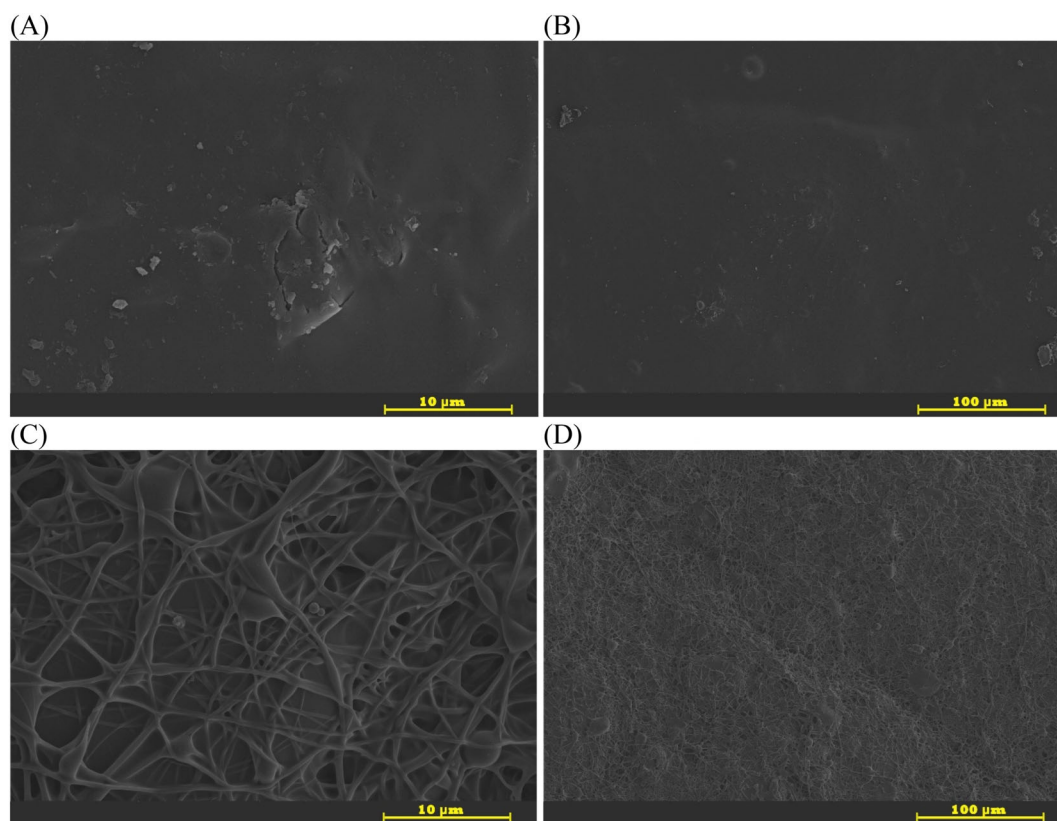


FIGURE 5 SEM images of (A, B) PVA-filled, (C, D) Nafion-filled PVA/Nafion nanofibrous membranes after methanol solution treatment.

TABLE 3 IEC, methanol permeability and proton conductivity properties of PVA/Nafion nanofibrous composite membranes.

|                   | Thickness, mm | IEC, mmol g <sup>-1</sup> | Proton conductivity, Scm <sup>-1</sup> |        |        |        | Methanol permeability, cm <sup>2</sup> s <sup>-1</sup> | Selectivity, ×10 <sup>-3</sup> Scm <sup>-3</sup> s |
|-------------------|---------------|---------------------------|--|--------|--------|--------|--|--|
|                   |               |                           | 40 RH%                                 | 60 RH% | 80 RH% | 100RH% |  |  |
| PVA/Nafion        | 0.11          | 0.88                      | 0.0                                    | 0.0    | 0.0    | 0.0    | 3.8 × 10 <sup>-5</sup>                                 | 0.0  |
| PVA/Nafion+PVA    | 0.12          | 1.28                      | 0.0                                    | 0.0    | 2.2    | 12.4   | 1.5 × 10 <sup>-6</sup>                                 | 8.3  |
| PVA/Nafion+Nafion | 0.12          | 1.67                      | 0.0                                    | 0.0    | 2.7    | 9.1    | 1.3 × 10 <sup>-5</sup>                                 | 0.7  |
| Nafion 115        | 0.13          | 0.96                      |  |        |        | 70.1   | 2.4 × 10 <sup>-6</sup>                                 | 29.2   |

compared to PVA coating. In FTIR analysis (Figure 2), the higher intensity of the peak at 1054 cm<sup>-1</sup> attributed to the sulfonic acid groups in the Nafion-filled membrane was also confirmed.

Proton transfer occurs through two mechanisms: the Grotthuss mechanism, in which protons hop from one anionic group to the other one through hydrogen bonds, and the vehicular mechanism, in which protons diffuse with water molecules.<sup>47</sup> Therefore, proton transport depends on both the IEC and water content of a membrane. When comparing the proton conductivity performances of PVA/Nafion-based membranes, no proton conductivity values were obtained by neat PVA/Nafion nanofibers. It was thought that continuous proton

transfer channels could not be formed due to the extremely porous structure of PVA/Nafion nanofibers. Fortunately, proton conductivity was achieved as a result of the filling process, which eliminates the pores between the nanofibers. On the other hand, at lower relative humidity values no proton conductivity was observed even for filled membranes. It is known that the water content within the membrane is crucial for proton transfer and lower humidity values lead to lower proton conductivity values.<sup>48</sup> Peckham et al.<sup>49</sup> reported that low relative humidity values (i.e. <70 RH%) values led to a decrease in proton mobility, therefore, conductivity due to the less screening of the tethered sulfonic acid groups. In the case of produced PVA/Nafion membranes, PVA

fraction within the membranes increases the hydrophilic character and, therefore, the water uptake of the membrane. Under low relative humidity values, it was thought that the water in the membrane was retained by the PVA fraction and prevented the formation of connected water-saturated proton conduction channels. In other words, in these membranes with high hydrophilicity, proton conduction channels with water-filled pathways could be formed only after a certain relative humidity ratio, which was shown to be 80 RH%.

As IEC increases, water uptake and proton conductivity generally increase; however, this is not always the case. For example, in the study of Yuan et al.<sup>50</sup> it was mentioned that Nafion-PSU-PVA-10 membrane had lowest proton conductivity, although its IEC was higher than recast Nafion. Also, in the study of Rhim et al.<sup>39</sup> in which PVA membranes were cross-linked by sulfosuccinic acid, it was suggested that the increase in IEC is not always a primary factor to increase proton conductivity. Therefore, the microstructure of the membrane, which is strongly affected by the polymer structure that changes the formation of ionic channels and proton mobility is of great importance.<sup>51</sup> In the present study, increase in water uptake was not just related to the addition of sulfonic acid groups to the structure, but rather because of the hydrophilic PVA fraction in the structure. Therefore, the expected relationship between IEC and proton conduction was not also observed in the high humidity values. At 80 RH%, the Nafion-coated membrane, which also had higher IEC compared to PVA-filled one showed leastwise higher proton conductivity as expected. On the other hand, while at 100 RH%, the PVA-coated membrane showed higher proton conductivity, which was thought to be related to the higher water uptake capacity of the PVA-coated membrane. On the other hand, this high water uptake might be the reason for displayed lower proton conductivity compared to commercial Nafion membrane, although PVA/Nafion-based nanofibers had higher IEC. Indeed, in another study by Peckham et al.<sup>52</sup> it was reported that higher ion content has led to lower proton conductivity by the dilution of available protons due to very high water uptake.

Methanol permeability test results showed that neat PVA/Nafion nanofibers exhibited significantly high methanol permeation as expected due to the higher porosity of electrospun nanofibers. Nafion coating was also unsuccessful in terms of the improvement of the methanol permeability. Conversely, the application of PVA filling, as depicted in Figure 1, was shown to cover the membrane surface with a film layer, resulting in lower methanol permeability given to PVA's higher affinity for water than methanol.<sup>14</sup> It was shown that PVA/Nafion+PVA membranes had lower methanol permeability than commercial Nafion 115 membranes and although PVA/Nafion+PVA

membrane was thinner, methanol permeation was found to be comparable to that of Nafion 117 membrane (tested as  $1.22 \times 10^{-6} \text{ cm}^2\text{s}^{-1}$  by Mondal et al.<sup>53</sup> with 0.18 mm thickness).

The selectivity of the membranes is also reported in Table 3 and shown that PVA/Nafion+PVA had a higher selectivity than PVA/Nafion+Nafion, owing to its lower methanol permeability. In addition, this improvement reduced the performance difference with the commercial membrane.

It should be noted that, although the PVA/Nafion+PVA as a cheap alternative has a potential use, a high swelling of PVA coating can create disadvantages in terms of mechanical stability. On the other hand, considering its lower methanol permeability and adequate thermal stability a further improvement potential is still existing. Therefore, as a continuation of this study, which investigated to what extent the type of filler affected the resultant membrane properties, the investigation of methods such as further crosslinking, grafting, and possible additives to improve the proton conductivity and swelling degree of PVA coated PVA/Nafion membranes appears as a planned future study topic.

## 4 | CONCLUSION

PVA/Nafion nanofibers were electrospun, physically stabilized, filled with PVA or Nafion, and sulfonated to produce nanofibrous polymer electrolyte membranes. Membranes were characterized by SEM, TGA, and FTIR analyses. Morphology, stability, and technical properties such as IEC, proton conductivity, and methanol permeability of the resultant membranes were investigated and compared.

PVA and Nafion polymers were used for pore filling. SEM analysis showed that PVA application led to a smooth film formation on the membrane surface, while Nafion filling mostly penetrated into the nanofibrous structure. After hot water and methanol solution treatment, membranes were shown to preserve their nanofibrous structure. PVA-filled membranes had higher water swelling values. TGA indicated that the resultant membranes had adequate thermal stability.

Neat PVA/Nafion membranes showed no proton conductivity. Proton conductivity was displayed after filling with PVA or Nafion after higher relative humidity (>80 RH%). The proton conductivity of the nanofibrous membrane filled with PVA was found to be highest at 100% RH. In addition, the methanol permeability of this membrane was the lowest, which was lower than commercial Nafion membrane. Moreover, given the higher

proportion of PVA in the structure compared to Nafion (with approximately 25% Nafion and 75% PVA in the final membrane), it is anticipated that the resulting membranes will be more cost-effective.

In the ongoing studies, the effects of possible additives to improve the proton conductivity and water uptake of PVA-filled PVA/Nafion nanofibrous membranes were planned to be investigated. Also, fuel test performances and mechanical properties of the membranes of different thicknesses were included in future study plans.

## ACKNOWLEDGMENTS

The authors would like to gratefully acknowledge the financial support for this research received through Ege University, Scientific Research Projects Coordination Unit (Project no. FYL-2019-21411). A limited part of this study was presented in IITAS 2023, XVI<sup>th</sup> International Izmir Textile and Apparel Symposium, October 27-25, 2023, Izmir, Türkiye.

## CONFLICT OF INTEREST STATEMENT

The authors declared no potential conflicts of interest with respect to the research, authorship, and/or publication of this article.

## DATA AVAILABILITY STATEMENT


All data generated or analyzed during this study are included in this published article.

## ORCID

Mert Işıl原因  <https://orcid.org/0000-0001-5330-4057>

Ahmet Çay  <https://orcid.org/0000-0002-5370-1463>

Çiğdem Akduman  <https://orcid.org/0000-0002-6379-6697>

Emriye Perrin Akçakoca Kumbasar  <https://orcid.org/0000-0001-5295-9131>

Hasan Ertaş  <https://orcid.org/0000-0002-5539-3732>

## REFERENCES

- Siddik AB, Khan S, Khan U, Yong L, Murshed M. The role of renewable energy finance in achieving low-carbon growth: contextual evidence from leading renewable energy-investing countries. *Energy*. 2023;270:126864.
- Alghassab M. Quantitative assessment of sustainable renewable energy through soft computing: fuzzy AHP-TOPSIS method. *Energy Rep*. 2022;8:12139-12152.
- Altaf F, Gill R, Batool R, et al. Proton conductivity and methanol permeability study of polymer electrolyte membranes with range of functionalized clay content for fuel cell application. *Eur Poly J*. 2019;110:155-167.
- Lucia U. Overview on fuel cells. *Renew Sust Energy Rev*. 2014;30:164-169.
- Giorgi L, Leccese F. Fuel cells: technologies and applications. *Open Fuel Cells J*. 2013;6(1):1-20.
- Palanisamy G, Jung HY, Sadhasivam T, Kurkuri MD, Kim SC, Roh SH. A comprehensive review on microbial fuel cell technologies: processes, utilization, and advanced developments in electrodes and membranes. *J Clean Prod*. 2019;221:598-621.
- Bharti A, Natarajan R. Proton exchange membrane testing and diagnostics. In: Kaur G, ed. *PEM Fuel Cells: Fundamentals, Advanced Technologies, and Practical Application Proton Exchange Membrane Testing and Diagnostics*. Elsevier; 2022.
- Akel M, Üniğür Çelik S, Bozkurt A, Ata A. Nano hexagonal boron nitride–Nafion composite membranes for proton exchange membrane fuel cells. *Poly Compos*. 2016;37(2):422-428.
- Mollá S, Compañ V. Polyvinyl alcohol nanofiber reinforced Nafion membranes for fuel cell applications. *J Membrane Sci*. 2011b;372(1–2):191-200.
- Ercelik M, Ozden A, Devrim Y, Colpan CO. Investigation of Nafion based composite membranes on the performance of DMFCs. *Int J Hydrogen Energ*. 2017;42(4):2658-2668.
- Prapainainar P, Theampetch A, Kongkachuichay P, Laosiripojana N, Holmes SM, Prapainainar C. Effect of solution casting temperature on properties of nafion composite membrane with surface modified mordenite for direct methanol fuel cell. *Surf Coat Tech*. 2015;271:63-73.
- Xia R, Zhou H, Zhang Z, Wu R, Wu WP. Effects of loading conditions on the nanoindentation creep behavior of Nafion 117 membranes. *Polym Eng Sci*. 2018;58(11):2071-2077.
- Rao AS, Rashmi KR, Manjunatha DV, Jayarama A, Shastrimath VVD, Pinto R. Methanol crossover reduction and power enhancement of methanol fuel cells with polyvinyl alcohol coated Nafion membranes. *Mater Today-Proc*. 2019;35:344-351.
- DeLuca NW, Elabd YA. Nafion<sup>®</sup>/poly(vinyl alcohol) blends: effect of composition and annealing temperature on transport properties. *J Membrane Sci*. 2006;282(1–2):217-224.
- Wu L, Zhang Z, Ran J, Zhou D, Li C, Xu T. Advances in proton-exchange membranes for fuel cells: an overview on proton conductive channels (PCCs). *Phys Chem Chem Phys*. 2013;15(14):4870-4887.
- Şendil Ö, Samatya Yilmaz S, Yazici Ozcelik E, Uzuner H, Aytac A. Cross-linked electrospun polyvinyl alcohol/sodium caseinate nanofibers for antibacterial applications. *J Vinyl Addit Techn*. 2023;29(1):48-65.
- Elhami M, Habibi SA. Study on UV-protection property of poly(vinyl alcohol)-montmorillonite composite nanofibers. *J Vinyl Addit Techn*. 2021;27(1):89-96.
- Gundloori RV, Singam A, Killi N. Nanobased intravenous and transdermal drug delivery systems. In: Mohapatra SS, Rajan S, Dasgupta N, Mishra RK, Thomas S, eds. *Applications of Targeted Nano Drugs and Delivery Systems, Nanobased Intravenous and Transdermal Drug Delivery Systems*. Elsevier; 2019.
- Yao Y, Ji L, Lin Z, et al. Sulfonated polystyrene fiber network-induced hybrid proton exchange membranes. *ACS Appl Mater Inter*. 2011;3(9):3732-3737.
- Yao Y, Guo B, Ji L, et al. Highly proton conductive electrolyte membranes: fiber-induced long-range ionic channels. *Electrochem Commun*. 2011;13(9):1005-1008.
- Takemori R, Kawakami H. Electrospun nanofibrous blend membranes for fuel cell electrolytes. *J Power Sources*. 2010;195:5957-5961.
- Dong B, Gwee L, Salas-De La Cruz D, Winey KI, Elabd YA. Super proton conductive high-purity Nafion nanofibers. *Nano Lett*. 2010;10(9):3785-3790.

23. Laforgue A, Robitaille L, Mokrini A, Aji A. Fabrication and characterization of ionic conducting nanofibers. *Macromol Mater Eng*. 2007;292(12):1229-1236.
24. Lee KM, Choi J, Wycisk R, Pintauro PN, Mather P. Nafion nanofiber membranes. *ECs Transact*. 2009;25(1):1451-1458.
25. Bajon R, Balaji S, Guo SM. Electrospun Nafion nanofiber for proton exchange membrane fuel cell application. *J Fuel Cell Sci Tech*. 2009;6(3):310041-310046.
26. Sharma DK, Li F, Wu YN. Electrospinning of Nafion and polyvinyl alcohol into nanofiber membranes: a facile approach to fabricate functional adsorbent for heavy metals. *Colloid Surface A*. 2014;457(1):236-243.
27. Ballengee JB, Pintauro PN. Preparation of nanofiber composite proton-exchange membranes from dual fiber electrospun mats. *J Membrane Sci*. 2013;442:187-195.
28. Chen H, Snyder JD, Elabd YA. Electrospinning and solution properties of Nafion and poly(acrylic acid). *Macromolecules*. 2008;41(1):128-135.
29. Lin HL, Wang SH. Nafion/poly(vinyl alcohol) nano-fiber composite and Nafion/poly(vinyl alcohol) blend membranes for direct methanol fuel cells. *J Membrane Sci*. 2014;452:253-262.
30. Mollá S, Compañ V. Performance of composite Nafion/PVA membranes for direct methanol fuel cells. *J Power Sources*. 2011;196(5):2699-2708.
31. Seino F, Konosu Y, Ashizawa M, Kakihana Y, Higa M, Matsumoto H. Polyelectrolyte composite membranes containing electrospun ion-exchange nanofibers: effect of nanofiber surface charges on ionic transport. *Langmuir*. 2018;34(43):13035-13040.
32. Lin HL, Wang SH, Chiu CK, et al. Preparation of Nafion/poly(vinyl alcohol) electro-spun fiber composite membranes for direct methanol fuel cells. *J Membrane Sci*. 2010;365(1-2):114-122.
33. Zizhou RE, Çay A, Kumbasar EPA, Çolpan CÖ. Production of poly(vinyl alcohol)/Nafion® nanofibers and their stability assessment for the use in direct methanol fuel cells. *J Ind Text*. 2021;50(6):773-793.
34. Çay A, Miraftab M. Properties of electrospun poly(vinyl alcohol) hydrogel nanofibers crosslinked with 1,2,3,4-butanetetracarboxylic acid. *J Appl Polym Sci*. 2013;129:3140-3149.
35. Çay A, Miraftab M, Akçakoca Kumbasar EP. Characterization and swelling performance of physically stabilized electrospun poly(vinyl alcohol)/chitosan nanofibers. *Eur Polym J*. 2014;61:253-262.
36. Mollá S, Compañ V, Gimenez E, Blazquez A, Urdanpilleta I. Novel ultrathin composite membranes of Nafion/PVA for PEMFCs. *Int J Hydrogen Energ*. 2011;36(16):9886-9895.
37. Kim YS, Hickner MA, Dong L, Pivovar BS, McGrath JE. Sulfonated poly(arylene ether sulfone) copolymer proton exchange membranes: composition and morphology effects on the methanol permeability. *J Membrane Sci*. 2004;243:317-326.
38. Kuwertz R, Kirstein C, Turek T, Kunz U. Influence of acid pretreatment on ionic conductivity of Nafion® membranes. *J Membrane Sci*. 2016;500:225-235.
39. Rhim JW, Park HB, Lee CS, Jun JH, Kim DS, Lee YM. Cross-linked poly(vinyl alcohol) membranes containing sulfonic acid group: proton and methanol transport through membranes. *J Membrane Sci*. 2004;238(1-2):143-151.
40. Lu J, Tang H, Xu C, Jiang SP. Nafion membranes with ordered mesoporous structure and high water retention properties for fuel cell applications. *J Mater Chem*. 2012;22:5810-5819.
41. Liang Z, Chen W, Liu J, et al. FT-IR study of the microstructure of Nafion® membrane. *J Membrane Sci*. 2004;233:39-44.
42. Kim DS, Guiver MD, Nam SY, et al. Preparation of ion exchange membranes for fuel cell based on crosslinked poly(vinyl alcohol) with poly(styrene sulfonic acid-co-maleic acid). *J Membrane Sci*. 2006;281:156-162.
43. Shin SJ, Balabanovich AI, Kim H, Jeong J, Song J, Kim HT. Deterioration of Nafion 115 membrane in direct methanol fuel cells. *J Power Sources*. 2009;191:312-319.
44. Peng Z, Kong LX. A thermal degradation mechanism of polyvinyl alcohol/silica nanocomposites. *Polym Degrad Stabil*. 2007;92:1061-1071.
45. Miraftab M, Saifullah AN, Çay A. Physical stabilisation of electrospun poly(vinyl alcohol) nanofibres: comparative study on methanol and heat-based crosslinking. *J Mater Sci*. 2015;50:1943-1957.
46. Al Munsur AZ, Goo BH, Kim Y, et al. Nafion-based proton-exchange membranes built on cross-linked semi-interpenetrating polymer networks between poly(acrylic acid) and poly(vinyl alcohol). *ACS Appl Mater Interfaces*. 2021;13:28188-28200.
47. Ng WW, Thiam HS, Pang YL, Lim YS, Wong J. Self-healable Nafion-poly(vinyl alcohol)/phosphotungstic acid proton exchange membrane prepared by freezing-thawing method for direct methanol fuel cell. *J Solid State Electr*. 2023;27:1477-1492.
48. Liu L, Chen W, Li Y. An overview of the proton conductivity of nafion membranes through a statistical analysis. *J Membrane Sci*. 2016;505:1-9.
49. Peckham TJ, Schmeisser J, Holdcroft S. Relationships of acid and water content to proton transport in statistically sulfonated proton exchange membranes: variation of water content via control of relative humidity. *J Phys Chem B*. 2008;112:2848-2858.
50. Yuan C, Li Q, Dong Y, et al. Click chemistry-based azide-substituted polysulfone/alkynyl-substituted sulfonated polyvinyl alcohol/nafion blend membranes for direct methanol fuel cells. *J Polym Sci*. 2024;62:3237-3257.
51. Yang Y, Lu F, Gao X, Xie S, Sun N, Zheng L. Effect of different ion-aggregating structures on the property of proton conducting membrane based on polyvinyl alcohol. *J Membrane Sci*. 2015;490:38-45.
52. Peckham TJ, Schmeisser J, Rodgers M, Holdcroft S. Main-chain, statistically sulfonated proton exchange membranes: the relationships of acid concentration and proton mobility to water content and their effect upon proton conductivity. *J Mater Chem*. 2007;17:3255-3268.
53. Mondal S, Soam S, Kundu PP. Reduction of methanol crossover and improved electrical efficiency in direct methanol fuel cell by the formation of a thin layer on Nafion 117 membrane: effect of dip-coating of a blend of sulphonated PVdF-co-HFP and PBI. *J Membrane Sci*. 2015;474:140-147.

**How to cite this article:** Işıl M, Çay A, Akduman Ç, Kumbasar EPA, Ertaş H. Effects of filler material on the characteristics of electrospun polyvinyl alcohol/Nafion nanofibrous membranes. *Polym Eng Sci*. 2024;1-13. doi:10.1002/pen.26943